Analysis of optimal bolometer sensitivity with linear approximation

Jin-Shown Shie, Yeong-Maw Chen and Chin-Shone Sheen

Institute of Electro-Optical Engineering, National Chiao Tung University
1001 Ta Hsueh Road, Hsinchu, Taiwan, R.O.C.

ABSTRACT

In this report, a general analysis for optimal sensitivity of microbolometers with constant-current operation is described. Using a linear approximation of bolometer resistance with respect to temperature variation, close-form solution of the optimal condition can be obtained among a set of operational variables and device parameters, including the sensor resistance, TCR, thermal conductance and bias current or voltage. The solution is close to that calculated by the exact numerical method. It is found that, under constant-current operation, a stable (relative) maximum of the sensor responsivity can only be obtained for NTCR, bolometers. The maximum sensitivity may reach 10^6 V/W with practical parameters considered for uncooled FPA bolometers working in vacuum. At such condition, a thermal detector may perform a D^* value close to the BLIP condition, if it has a radiation-loss-limited feature. Also, a large-area single bolometer operated in the atmosphere may have a performance comparable to that of the present commercial pyroelectric detectors.

Keywords: bolometer, sensitivity, optimization analysis, constant-current bias

1. INTRODUCTION

In recent years, uncooled thermal detectors for far-infrared sensing have been developed rapidly.[1-6] These detectors were fabricated with high yield utilizing surface micromachining technology on silicon substrate. The tiny microsensors of 2D-array, each has extremely small values of thermal parameters, therefore can be built, and high sensitivity far beyond the performance of conventional thermal detectors can be demonstrated.

However, the performance of a micro-bolometer depends on many working variables and parameters, which are related to material, circuit, device configuration as well as application specifications. They are also related to each other, making the optimal design of a bolometer function much more complicate than its apparent feature as a temperature-sensitive resistor. In the past, many theories had been reported on analyzing the maximal bolometer sensitivity,[7-11] but none is believed to be the general case.

In this report, the problem is considered from a broader aspect to include all influential factors, explicitly or implicitly. Constant-current bias circuit is used in the analysis as an illustration of methodology.

0-8194-2127-8/96/$6.00

2. SENSITIVITY WITH CONSTANT-CURRENT OPERATION

2.1 Bolometer resistance

A bolometer is a certain kind of temperature sensitive resistor. For metal-film type, the resistance at temperature T can be expressed as a series of temperature,

$$R_s = R_0[1 + a_1(T - T_0) + a_2(T - T_0)^2 + \ldots]. \quad (1)$$

Here R_0 is the resistance measured at a reference temperature T_0, and a_1, a_2 ... are the temperature coefficients corresponding to the various orders. For thermistor type, the resistance is generally expressed by

$$R_s = R_0 e^{[B(\frac{1}{T} - \frac{1}{T_0})]}, \quad (2)$$

with a positive material constant B. If the sensor temperature $T \approx T_0$, then Eq.(2) can be expanded by Taylor's series into

$$R_s = R_0[1 - \frac{B}{T_0^2}(T - T_0) + (\frac{B}{T_0^3} + \frac{B^2}{2T_0^4})(T - T_0)^2 + \ldots]. \quad (3)$$

This equation has the same formula as Eq.(1). For estimation, if B = 3000 K and T_0 = 300 K, then $a_1 = -B/T_0^2 = -3.3\times10^{-2}$ /K and $a_2 = B/T_0^3 + B/2T_0^4 = 1.3\times10^{-3}$ /K^2. The series converges rapidly, and Eq.(1) can be concluded as a general form of bolometer resistance. This equation can be re-formulated into

$$R_s = R_0[1 + a(T - T_0)], \quad (4)$$

with

$$a(T) = a_1 + a_2(T - T_0) + \ldots \quad (5)$$

being a function of temperature.

2.2 Thermal responsivity

The electro-thermal behavior of a bolometer can be expressed by a lumped heat-flow equation,

$$H\frac{dT}{dt} + G(T - T_a) = P + \varepsilon\Phi. \quad (6)$$

Here T is the sensor temperature, and T_a the ambient temperature. ε, H and G are the sensor emissivity, thermal capacitance and conductance, respectively. Also, P is the electrical self-heating power and Φ is the optical input power. For simplicity of analysis, we will assume that T_0 in Eq.(1) is at the ambient temperature T_a, which is maintained at constant.

In d.c. steady-state (static) condition, $\Phi = \Phi_0$ and $T = T_x$, both are at constant, hence the heat-flow equation becomes

$$G(T_x - T_a) = GT_{xa} = P_x + \varepsilon\Phi_0 = I_0^2 R_{sx} + \varepsilon\Phi_0, \quad (7)$$

where $T_{xa} = T_x - T_a$, the excess sensor temperature above the ambient, while P_x and R_{sx} denote the self-heating power and sensor resistance at the operation temperature T_x, respectively.

In the following, we use harmonic analysis for a.c. steady-state solution. Let $\Phi = \Phi_0 + \Phi_\omega e^{j\omega t}$ and $T = T_x + \theta$, and put them into Eq.(6). With the help of Eq.(7) one obtains

$$H\frac{d\theta}{dt} + G\,\theta = \left.\frac{\partial P}{\partial T}\right|_{T_x} \theta + \varepsilon\Phi_\omega e^{j\omega t}, \quad (8)$$

to the first-order approximation for the perturbed temperature θ. Define the effective thermal conductance for constant-current operation by

$$G_{eff} = G - \left.\frac{\partial P}{\partial T}\right|_{T_x} = G - I_0^2 \left.\frac{\partial R_s}{\partial T}\right|_{T_x} = G - I_0^2\,\alpha_x\,R_{sx}, \quad (9)$$

where α_x is the temperature coefficient of resistance (TCR) at operating temperature T_x which is defined as

$$\alpha_x \equiv \frac{1}{R_s}\left.\frac{dR_s}{dT}\right|_{T_x}. \quad (10)$$

Obviously, Eq.(8) has a solution for the thermal responsivity

$$|S_T| = \left|\frac{dT}{d\Phi}\right| = \left|\frac{\theta}{\Phi_\omega e^{j\omega t}}\right|$$

$$= \frac{\varepsilon}{G_{eff}\sqrt{1+\omega^2\tau_{eff}^2}} = \frac{S_{T0}}{\sqrt{1+\omega^2\tau_{eff}^2}}. \quad (11)$$

The effective thermal time constant $\tau_{eff} = H/G_{eff}$, and the flatband responsivity $S_{T0} = \varepsilon/G_{eff}$.

The voltage responsivity of the bolometer, S_V, is related to its electrical, material and thermal properties, given by

$$S_V \equiv \left|\frac{dV_o}{d\Phi}\right| = \left|\frac{dV_o}{dR_s}\right| \times \left|\frac{dR_s}{dT}\right| \times \left|\frac{dT}{d\Phi}\right|. \quad (12)$$

It is easy to prove that, for constant-current circuit, S_V has a formula[12]

$$S_V = \frac{\varepsilon I_0 \alpha_x R_{sx}}{G - I_0^2 \alpha_x R_{sx}} \frac{1}{\sqrt{1+\omega^2\tau_{eff}^2}} = \frac{S_0}{\sqrt{1+\omega^2\tau_{eff}^2}}, \tag{13}$$

with the flatband responsivity

$$S_0 = \frac{\varepsilon I_0 \alpha_x R_{sx}}{G - I_0^2 \alpha_x R_{sx}}. \tag{14}$$

One should note that S_0 contains many device variables. Certain relationships between them have to be found for optimizing the quantity.

3. OPTIMIZATION

The optimization of S_0 is under the constraint of Eq.(7). Hence not all parameters can be adjusted independently. Here we choose the bias current I_0 as the independent variable, which is also contained implicitly in quantities T_x, α_x, and R_{sx}. If G is assumed to be weakly dependent on the sensor temperature, then it is easy to prove that the optimal condition is given by

$$\frac{dS_0}{dI_0} \equiv \frac{\partial S_0}{\partial I_0} + \frac{\partial S_0}{\partial T_x}\frac{dT_x}{dI_0} = 0. \tag{15}$$

From Eq.(14),

$$\frac{\partial S_0}{\partial I_0} = \frac{\varepsilon \alpha_x R_{sx}}{(G - I_0^2 \alpha_x R_{sx})^2}(G + I_0^2 \alpha_x R_{sx}), \tag{16}$$

$$\frac{\partial S_0}{\partial T_x} = \frac{\varepsilon I_0 G}{(G - I_0^2 \alpha_x R_{sx})^2}\frac{d(\alpha_x R_{sx})}{dT_x}, \tag{17}$$

and

$$\frac{d(\alpha_x R_{sx})}{dT_x} = \alpha_x(\alpha_x + \frac{1}{\alpha_x}\frac{d\alpha_x}{dT_x})R_{sx} = \alpha_x \gamma R_{sx}, \tag{18}$$

where

$$\gamma = \alpha_x + \frac{1}{\alpha_x}\frac{d\alpha_x}{dT_x}. \tag{19}$$

Also from Eq.(7) of the static balance condition,

$$G = 2I_0 R_{sx}\frac{dI_0}{dT_x} + I_0^2\frac{dR_{sx}}{dT_x} = 2I_0 R_{sx}\frac{dI_0}{dT_x} + I_0^2 \alpha_x R_{sx}, \tag{20}$$

or equivalently,

$$\frac{dT_x}{dI_0} = \frac{2I_0 R_{sx}}{G - I_0^2 \alpha_x R_{sx}}. \tag{21}$$

Substituting Eqs.(16), (17) and (21) into Eq.(15), one obtains a simplified relationship,

$$G^2 - I_0^4 \alpha_x^2 R_{sx}^2 + 2GI_0^2 \gamma R_{sx} = 0, \tag{22}$$

for the optimal sensitivity. Use Eq.(7) again, it turns out

$$G^2 - \alpha_x^2 (GT_{xa} - \varepsilon\Phi_0)^2 + 2G\gamma(GT_{xa} - \varepsilon\Phi_0) = 0, \tag{23}$$

or

$$T_{xa}^2 - 2\left(\frac{\varepsilon\Phi_0}{G} + \frac{\gamma}{\alpha_x^2}\right)T_{xa} + \frac{\varepsilon\Phi_0}{G}\left(\frac{\varepsilon\Phi_0}{G} + \frac{2\gamma}{\alpha_x^2}\right) - \frac{1}{\alpha_x^2} = 0. \tag{24}$$

This equation can only be solved when α_x and γ are explicitly expressed in terms of temperature.

4. LINEAR APPROXIMATION

To explore the analysis further, approximation of linear dependence of R_s on temperature is assumed. This means $a = a_1$ is a constant. By the definition of Eq.(10), the TCR at T_x reads

$$\alpha_x = \frac{a_1}{1 + a_1(T_x - T_a)} = \frac{a_1}{1 + a_1 T_{xa}}. \tag{25}$$

Substituting Eq.(25) into Eq.(19), one can find that γ is vanished accordingly. Note that a_1 is the measured constant referred to the ambient temperature T_a, which has been assumed fixed as mentioned before. With this assumption, Eq.(22) becomes

$$G = \pm I_0^2 \alpha_x R_{sx}. \tag{26}$$

One should note that since G can not be negative, therefore "+" term is for PTCR and "-" term is for NTCR. However, by Eq.(9), the effective thermal conductance, G_{eff}, is reduced to zero for PTCR case. This results in an unstable sensitivity, according to Eq.(11). Therefore, the positive term is not the solution and PTCR sensor has no stable maximum under constant-current bias circuit. The excess sensor temperature at $G = -I_0^2 \alpha_x R_{sx}$ condition for NTCR then read

$$T_{xa} = \frac{\varepsilon\Phi_0}{2G} - \frac{1}{2a_1}, \tag{27}$$

and the maximal sensitivity can be expressed by

$$S_{0m} = \frac{\varepsilon}{2I_0} = \frac{\varepsilon}{2}\sqrt{\frac{|\alpha_x| R_{sx}}{G}} = \frac{\varepsilon}{2}\sqrt{\frac{|a_1| R_0}{G}}. \tag{28}$$

The last equality can be derived from the definition of TCR in Eq.(10) for the linear temperature approximation. In fact, the solution of the optimal condition can be obtained from Eq.(14) more directly, if the invariant property, $\alpha_x R_{sx} = a_1 R_0$, is noticed. Fig.1 shows the S_0-I_0 plot with G as parameter for a thermistor sensor under constant-current operation, according to the linear approximation. The results are smaller but close to the numerical calculations using the precise thermistor resistance of Eq.(2). The responsivity can be as high as 10^6 V/W at extremely low value of G. The maximal sensitivities are shown in Fig.2 with $\Phi_0 = 0$ and 1μW (dotted curves). Exact solutions are also shown by solid curves for comparison.

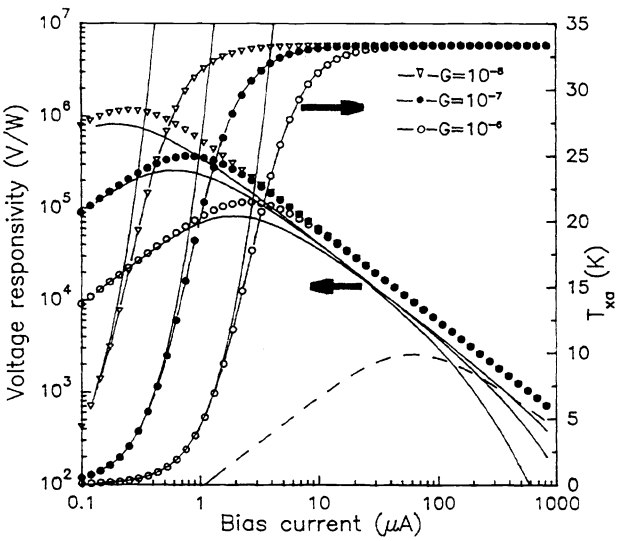

Fig. 1 The S_o-I_o and T_{xa}-I_0 plots with G as the parameter. Curves with symbols are solutions for linear approximation, and solid lines are the exact numerical calculations. The device parameters: R_a=5MΩ, T_a=300K, α=-3%, ε=0.6.

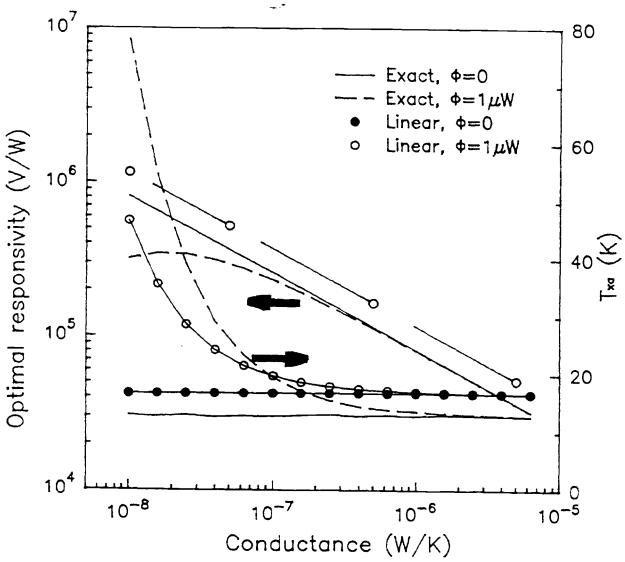

Fig. 2 The S_{om}-G and T_{xa}-G plots with different Φ_0. The exact solutions have lower S_{om} than that given by linear approximation.

5. DISCUSSIONS

In Fig.1, the excess operation temperature T_{xa} is also plotted. For linear approximation, the excess temperatures for different values of thermal conductance all saturate at high current region. However, these results are quite different from that calculated with exact formula of thermistor resistance of Eq.(2). Nevertheless, at optimal points the deviations are small except at very low value of G. This can be understand from Fig.3 in which both the power dissipation and generation on the device are plotted as function of the device temperature T_x. The solutions of T_{xa} are given by the cross points of the two curves. One can see that the cross point (×) moves faster to the high temperature regime when the thermal conductance decreases in the exponential form of thermistor resistance (solid curve) than in the linear form (broken curve). Therefore, we conclude that linear approximation is not accurate enough to predicate the operation temperature of thermistor device at low G. However, T_{xa} is lower than expected in real situation. Since at very low G, the device is

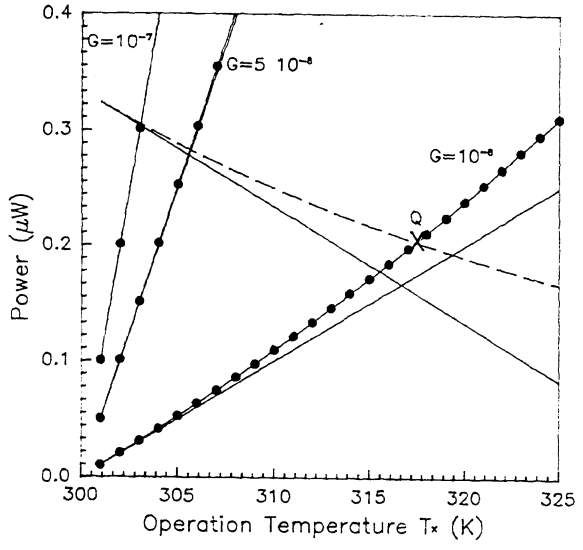

Fig. 3 Interpretation of operation temperature T_{xa} of NTCR bolometers. Where T_a=300K, I_0=0.258μA, R_a=5MΩ, α=-3% are used.

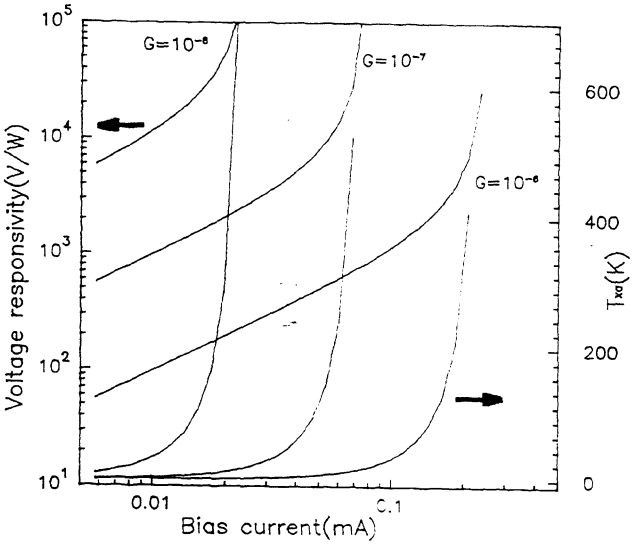

Fig. 4 The S_0-I_0 and T_{xa}-I_0 plots of PTCR bolometers with constant-current operation. Thermal run-away due to the self-feed-back heating is observed for T_{xa}curve.

generally radiation-loss-limited[13] which is strongly temperature dependent, not a constant as we have assumed. The increased loss conductance at higher temperature as shown by the solid-dotted curve of G = 10^{-8} makes the cross point (denoted Q in Fig.3) downward to certain extent. It is interesting to note that for PTCR bolometers, the self-heating power should has a positive slope in Fig.3, therefore the cross-point temperature will vary much widely than NTCR device for constant-current circuit, which is much more unstable.

The unstable condition of the maximal sensitivity for PTCR is Eq.(26) mathematically is an absolute maximum, which runs the device into thermal run-away destruction by its own self-heating. This is plotted in Fig.4. For this reason, the PTCR device can only be biased and read with pulse method.[4] However, when a constant-voltage bias circuit is used for bolometers, the conjugate condition of constant-current operation can be obtained, where the previous analyzed results between PTCR and NTCR devices are reversed.

In a commercial single pyroelectric detector, the device has a larger area of about 1 mm^2 and works in atmospheric ambient.[14] The loss conductance G is thus mainly contributed by the gaseous conductance, according to our previous reports.[13,15] With the same G as single pyroelectric detector, the bolometer has a maximal sensitivity of about 2600 V/W which is shown in the lowest curve (broken line) of Fig.1 with a -3%/K TCR and a 5 MΩ resistance of material constants. This value of voltage responsivity is comparable to that of the present low-cost pyroelectric detector.[14] However, manufacturing of this kind of bolometers with micromachining technology is much more easy by batch production, and the cost is even lower.

When the linear approximation is effective, and if the detector performance is Johnson-noise-limited, then the normalized detectivity at optimal condition can be written as

$$D^* = \frac{\sqrt{A_d \Delta f}}{NEP} = \frac{S_{0m}}{v_n}\sqrt{A_d \Delta f}$$

$$= \frac{\varepsilon}{2}\sqrt{\frac{|\alpha_x| R_{sx} / G}{4kT_x R_{sx} \Delta f}}\sqrt{A_d \Delta f} = \frac{\varepsilon}{2}\sqrt{\frac{|\alpha_x|}{4kT_x G_0}} \qquad (29)$$

with $G_0 = G/A_d$, the heat-loss conductance per unit area. If the device has a radiation-loss-limited feature, then[15]

$$G_0 = 2\varepsilon\sigma(T_x^2 + T_a^2)(T_x + T_a) \qquad (30)$$

and

$$D^* = \frac{1}{2}\sqrt{\frac{\varepsilon|\alpha_x|}{8\sigma k T_x (T_x^2 + T_a^2)(T_x + T_a)}} \qquad (31)$$

which is independent of detector area A_d. A practical estimation, with α_x = -3%/K, $T_x \approx T_a$ = 300 K, and ε = 0.6, $D^* \approx 4\times10^{10}$. This value is twice of the theoretical BLIP D^*.[16] Therefore the device can reach a performance of physical limit.

6. CONCLUSIONS

The performance of microbolometers has been analyzed theoretically. Stable (relative) maximum of the device voltage responsivity can be rationalized into a governing equation. A concise close-form solution can be obtained for the linear approximation of the bolometer resistance. Very high responsivity up to 10^6 V/W can be obtained theoretically at the optimum, at which the theoretical BLIP D^* performance with practical device parameters is also possible.

7. ACKNOWLEDGMENTS

The authors wish to thank the National Science Council of the Republic of China for financial support under project contract No. NSC-85-2215-E-009-040.

8. REFERENCES

1. R.E. Flannery and J.E. Miller, "Status of uncooled infrared imagers," *SPIE Proceedings*, Vol. 1689, pp. 379-395, 1992.

2. R.A. Wood, "Uncooled thermal imaging with monolithic silicon focal planes," *SPIE Proceedings*, Vol. 2020, pp. 322-329, 1993.

3. W.G. Baer, T. Hull, K.D. Wise, K. Najafi and Kensall D. Wise, "A multiplexed silicon infrared thermal imager," *The Technical Digest of Transducers'91*, pp. 631-634, 1991.

4. A. Tanaka, S. Matsumoto, N. Tsukamoto, S. Itoh, T. Endoh, A. Nakazoto, Y. Kumazawa, M. Hijikawa, H. Gotoh, T. Tanaka and N. Teranishi, "Silicon IC process compatible bolometer infrared focal plane array," *Tech. Digest, The 8th Int. Conf. on Solid-State Sensors and Actuators and Eurosensors IX, Stockholm, Sweden*, pp. 632-635, June 1995.

5. J.S. Shie and P.K. Weng, "Design considerations of metal-film bolometer with micromachined floating membrane," *Sensors and Actuators*, Vol. A33, pp. 183-189, 1992.

6. T. Mori, T. Kudoh, K. Komatsu and M. Kimura, "Vacuum-encapsulated thermistor bolometer type miniature infrared sensor," *IEEE Proc. MEMS*, pp. 257-262, Jan. 1994.

7. R.C. Jones, "The general theory of bolometer performance," *J. Opt. Soc. Am.*, Vol. 43, pp. 1-14, Jan. 1953.

8. J.C. Mather, "Bolometers: ultimate sensitivity, optimization, and amplifier coupling," *Appl. Opt.*, Vol. 23, pp. 584-588, Feb. 1984.

9. T.P. Vogl, G.A. Shifrin and B.J. Leon, "Generalized theory of metal-film bolometers," *J. Opt. Soc. Am.*, Vol. 52, pp. 957-964, Sep. 1962.

10. E.M. Wormser, "Properties of thermistor infrared detectors," *J. Opt. Soc. Am.*, Vol. 43, pp. 15-21, Jan. 1953.

11. P.L. Richards, "Bolometers for infrared and millimeter waves," *J. Appl. Phys.*, Vol. 76, pp. 1-24, July 1994.

12. Y.M. Chen, J.S. Shie and T. Hwang, "Parameter extraction of resistive thermal sensors," to be published in *Sensors and Actuators*.

13. J.S. Shie, B.C.S. Chou and Y.M. Chen, "High performance Pirani vacuum gauge," *J. Vac. Sci. Technol.*, Vol. A13, pp. 2972-2979, 1995.

14. Opto Tech Corporation Catalog, Hsinchu Science-based Industrial Park, Taiwan.

15. P.K. Weng and J. S. Shie, "Micro-Pirani vacuum gauge," *Rev. Sci. Instrum.*, Vol. 65, pp. 492-499, 1994.

16. R.H. Kingston, *Detection of optical and infrared radiation*, Ch. 7, Springer, New York, 1978.